Journal of Medicinal Chemistry

Additional resources and features associated with this article are available within the HTML version:

- Supporting Information
- Access to high resolution figures
- Links to articles and content related to this article
- Copyright permission to reproduce figures and/or text from this article

View the Full Text HTML

The Identification of 2-(1*H*-Indazol-4-yl)-6-(4-methanesulfonyl-piperazin-1-ylmethyl)-4-morpholin-4-yl-thieno[3,2-*d*]pyrimidine (GDC-0941) as a Potent, Selective, Orally Bioavailable Inhibitor of Class I PI3 Kinase for the Treatment of Cancer[†]

Adrian J. Folkes,*,[‡] Khatereh Ahmadi,[‡] Wendy K. Alderton,[‡] Sonia Alix,[||] Stewart J. Baker,[‡] Gary Box,[||] Irina S. Chuckowree,[‡] Paul A. Clarke,[||] Paul Depledge,[‡] Suzanne A. Eccles,[||] Lori S. Friedman,[§] Angela Hayes,[||] Timothy C. Hancox,[‡] Arumugam Kugendradas,[‡] Letitia Lensun,[‡] Pauline Moore,[‡] Alan G. Olivero,[§] Jodie Pang,[§] Sonal Patel,[‡] Giles H. Pergl-Wilson,[‡] Florence I. Raynaud,[||] Anthony Robson,[‡] Nahid Saghir,[‡] Laurent Salphati,[§] Sukhjit Sohal,[‡] Mark H. Ultsch,[§] Melanie Valenti,[||] Heidi J.A. Wallweber,[§] Nan Chi Wan,[‡] Christian Wiesmann,[§] Paul Workman,[||] Alexander Zhyvoloup,[‡] Marketa J. Zvelebil,[⊥] and Stephen J. Shuttleworth[‡]

Piramed Pharma, 957 Buckingham Avenue, Slough, Berks SL1 4NL, United Kingdom, Genentech, Inc., 1 DNA Way, South San Francisco, California 94080, Cancer Research UK Centre for Cancer Therapeutics, The Institute of Cancer Research, Haddon Laboratories, Sutton, Surrey, SN2 5NG, United Kingdom and Breakthrough Breast Cancer Research Centre, The Institute of Cancer Research, London, SW3 6JB, United Kingdom

Received March 17, 2008

Phosphatidylinositol-3-kinase (PI3K) is an important target in cancer due to the deregulation of the PI3K/Akt signaling pathway in a wide variety of tumors. A series of thieno[3,2-*d*]pyrimidine derivatives were prepared and evaluated as inhibitors of PI3 kinase p110α. The synthesis, biological activity, and further profiling of these compounds are described. This work resulted in the discovery of **17**, **GDC-0941**, which is a potent, selective, orally bioavailable inhibitor of PI3K and is currently being evaluated in human clinical trials for the treatment of cancer.

Introduction

Phosphatidylinositol-3-kinases (PI3Ks)[a] are lipid kinases that catalyze the phosphorylation of the 3-hydroxyl position of phosphatidylinositides.[1,2] To date, a total of eight PI3 kinases have been identified, which are divided into classes IA, 1B, II, and III on the basis of sequence homology and substrate preference. The PI3K superfamily also includes the Class IV PIK related enzyme family of protein kinases including mTOR, ATM, ATR, and DNA-PK. The class IA subgroup consists of p110α, p110β, and p110δ subtypes, and these primarily generate phosphatidylinositol 3,4,5-triphosphate (PI(3,4,5)P$_3$), which is a second messenger that facilitates activation of the downstream kinase Akt.[3] The consequences of biological activation of Akt include tumor progression, proliferation, survival, growth, invasion, angiogenesis, and metastasis, and there is significant evidence suggesting that the PI3K/Akt pathway is deregulated in many human cancers.[3] Furthermore, the gene encoding the p110α subunit, *PIK3CA*, is amplified and overexpressed in several ovarian cancer cell lines[4] and is mutated in a wide variety of other cancers including colorectal, glioblastoma, and gastric cancers.[4–7] PI3K signaling is negatively regulated by the dual phosphatase PTEN, which is one of the most commonly mutated
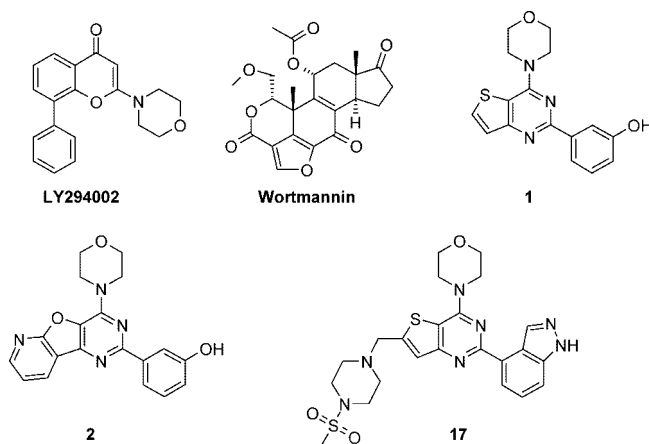

Figure 1. Structures of PI3K Inhibitors.

proteins in human malignancy, providing further evidence of the role of the PI3K pathway in cancer.[8,9] In addition, persistent signaling through the PI3K/Akt pathway has been shown to be a major mechanism of resistance to chemotherapeutics as well as therapeutic agents targeting the epidermal growth factor receptor family.[10] Among patients treated with trastuzumab, activation of the PI3K pathway has been associated with resistance and poor prognosis.[11,12] Hence inhibition of PI3K, and in particular p110α, is a promising target for cancer treatment.[7,13]

Several inhibitors of PI3 kinase have been reported in the literature,[7,14] including wortmannin[15,16] and LY294002[17] (Figure 1). Both of these compounds have been widely used to elucidate the functional role of PI3K.[14] However, their toxicity and lack of selectivity with respect to targets other than class I PI3K family members have limited their therapeutic potential. More recently, Hayakawa et al. have reported the thieno[3,2-*d*]pyrimidine derivative **1**[18] and the pyrido[3′,2′:4,5]furo-{3,2-

---

Scheme 1[a]

[a] Reagents and conditions: (a) 3-OTBDMS phenyl boronic acid, NaHCO$_3$, H$_2$O, Pd(PPh$_3$)$_2$Cl$_2$, DME, reflux, 51%. (b) (i) nBuLi, THF, −78 °C; (ii) DMF, 99%. (c) (i) RR′NH, 1,2-DCE, Na(OAc)$_3$BH, AcOH; (ii) TBAF, THF. (d) (i) nBuLi, THF, −78 °C; (ii) MeI, 82%. (e) 3-Hydroxyphenyl boronic acid, NaHCO$_3$, H$_2$O, Pd(PPh$_3$)$_2$Cl$_2$, DME, reflux, 10%. (f) (i) nBuLi, THF, −78 °C; (ii) DMF, 77%. (g) RR′NH, 1,2-DCE, Na(OAc)$_3$BH, HC(OMe)$_3$. (h) **25**, MeCN, Na$_2$CO$_3$, H$_2$O, Pd(PPh$_3$)$_2$Cl$_2$, microwave, 130 °C, 20 min.

d}pyrimidine derivative **2**,[19] both potent inhibitors of PI3K p110α with significant antiproliferative activity in vitro. Whereas **2** demonstrated encouraging activity against several human tumor xenografts,[20] the poor pharmacokinetic profile of **1** precluded any further evaluation of this compound, as the half-life is less than 10 min following intraperitoneal administration in mice.[18] Although **2** has been more extensively profiled,[20,21] we viewed **1** as offering greater potential for further optimization due to the relatively low molecular weight (MW = 313) and the opportunity to substitute the 6- and 7- positions of the thieno[3,2-*d*]pyrimidine to improve multiple aspects of the compound, including physicochemical properties, metabolic stability, and potency. Consequently, **1** was chosen as the starting point for our medicinal chemistry efforts.

Herein we disclose the synthesis and biological evaluation of a series of thieno[3,2-*d*]pyrimidines that demonstrate potent inhibition of PI3K p110α, culminating in the discovery of **17** (**GDC-0941**).

Chemistry

The general synthetic routes used to prepare thieno[3,2-*d*]pyrimidine derivatives are outlined in the following schemes.

In Scheme 1, 2-chloro-4-morpholin-4-yl-thieno[3,2-*d*]pyrimidine **3**[22] was treated with 3-(*tert*-butyldimethylsilyloxy)phenyl boronic acid under Suzuki conditions to provide **4**. Lithiation of **4**, followed by the addition of DMF, gave the aldehyde **5** in 99% yield. Treatment of **5** with the appropriate amine using standard reductive amination conditions, followed by treatment with tetrabutyl ammonium fluoride, provided the phenolic derivatives **6**−**9**.

To prepare the 6-methyl derivative **11,** the lithium anion of **3** was quenched with methyl iodide to provide **10**. Reaction with 3-hydroxyphenyl boronic acid under Suzuki conditions provided the desired compound.

Also in Scheme 1, lithiation of **3** followed by the addition of DMF yielded the aldehyde **13**. Reductive amination of **13** using

the appropriate amine and sodium triacetoxyborohydride proceeded smoothly to yield compounds **14**−**15**. Finally, Suzuki coupling with 4-(4,4,5,5-tetramethyl-[1,3,2]dioxaborolan-2-yl)-1*H*-indazole **25** yielded compounds **16**−**17**.

Scheme 2 describes the initial route used for the preparation of indazole derivatives **20** and **22**. Palladium mediated treatment of 3-bromo-2-methyl-aniline with pinacol borane yielded 2-methyl-3-(4,4,5,5-tetramethyl-[1,3,2]dioxaborolan-2-yl)-phenylamine **18**. Reaction of **18** with **3** under Suzuki conditions yielded **19**. Cyclisation with isoamyl nitrite resulted in the desired 4-indazolyl derivative **20.** The isomeric 6-indazolyl derivative **22** was prepared in an analogous manner from 3-amino-4-methylbenzeneboronic acid.

4-(4,4,5,5-Tetramethyl-[1,3,2]dioxaborolan-2-yl)-1*H*-indazole **25**, which was a more versatile intermediate for the preparation of indazole derivatives, is prepared in three steps from 3-bromo-2-methyl aniline as shown in Scheme 3.

Results and Discussion

It has previously been reported[18] that the morpholino group on the related quinazoline template was critical for p110α inhibitory activity, with all modifications to this position resulting in large reductions in potency. Studies on analogues of LY294002 have also shown that the morpholino group is critical for potency,[17] suggesting that the morpholino groups in the quinazoline series and LY294002 interact with the PI3K in a similar manner. As it was believed that the morpholino group was optimal, this group was retained with all further derivatives described herein.

Our initial efforts focused on substitutions of the 6- and 7-positions of the thieno[3,2-*d*]pyrimidine ring, with the primary aim of maintaining potency while improving the metabolic stability and the solubility of the series. Substitution with a methyl group in the 6-position, compound **11**, was well tolerated, whereas the 7-Me derivative **12** showed a slight decrease in potency (Table 1). Taking into consideration the potential to block any metabolism at the

Scheme 2[a]
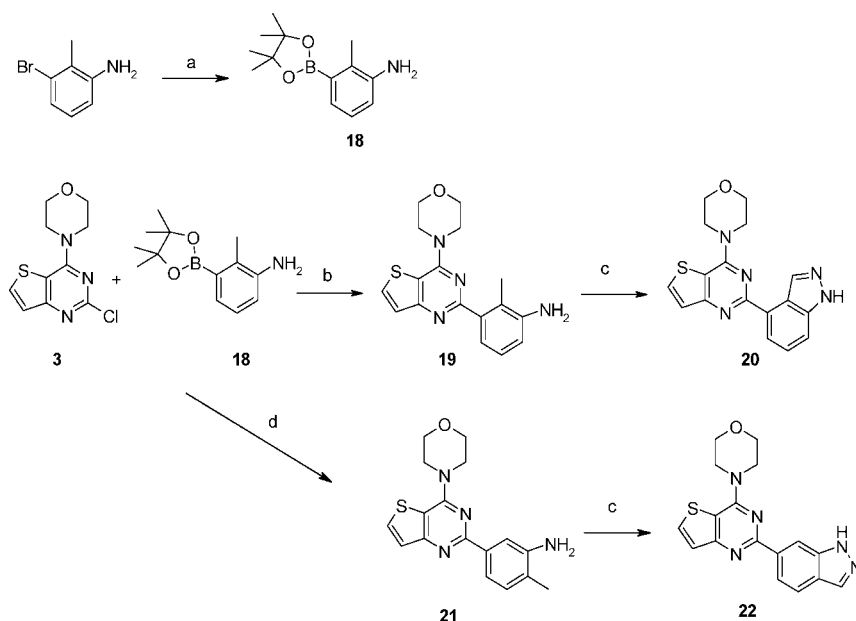
[a] Reagents and conditions: (a) pinacol borane, 2-dicyclohexylphosphinobiphenyl, Pd(OAc)$_2$, Et$_3$N, dioxane, 80° C, 85%; (b) DME, Na$_2$CO$_3$, H$_2$O, Pd(PPh$_3$)$_2$Cl$_2$, reflux, 69%; (c) isoamyl nitrite, CHCl$_3$, AcOH, 20% for **20**, 14% for **22**; (d) 3-amino-4-methylbenzene boronic acid, DME, Na$_2$CO$_3$, H$_2$O, Pd(PPh$_3$)$_2$Cl$_2$, reflux, 82%.

Scheme 3[a]
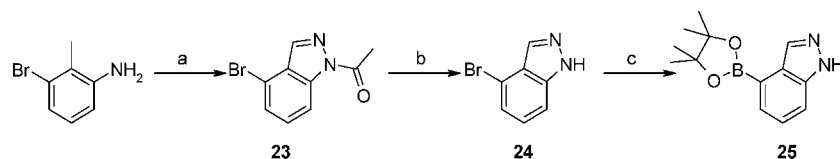
[a] Reagents and conditions: (a) (i) KOAc, Ac$_2$O; (ii) isoamyl nitrite, 18-crown-6, CHCl$_3$. (b) 6N HCl, MeOH, 86% from 3-bromo-2-methylaniline. (c) bis(pinacolato)diboron, PdCl$_2$(dppf)$_2$, KOAc, DMSO, 80 °C, 60%.

6-position of the thieno[3,2-*d*]pyrimidine ring, and the greater synthetic accessibility of this position, we concentrated our efforts to modifications at the 6- position.

The inhibitory activity of the compounds against p110α was measured using a radiometric scintillation proximity assay (SPA) with recombinant human p110α and 1 μM ATP. Inhibition of cell proliferation was measured using the Alamar Blue assay with the PTEN-null U87MG human glioblastoma cell line and with the *PIK3CA* mutant, PTEN mutant A2780 human ovarian cell line.[20,21]
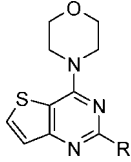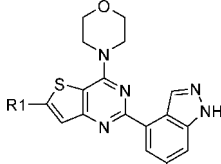
Figure 2. (a) ATP-binding site sequence alignment for p110α and p110γ, with key residues highlighted: hinge region Val (red), conserved Tyr and Asp located at the back end of the pocket (blue and green, respectively), and catalytic Lys (gray).[24–28] (b,c) **1** docked into the p110α homology model reveals key hydrogen bonds between the morpholine oxygen of **1** and Val851 in the hinge and between the exocyclic phenolic hydroxyl and Asp810, with the 6-position proton on thiophene ring extending out toward solvent.

Table 1. Inhibition of p110α Activity, Cancer Cell Proliferation, Metabolic Stability, and Oral Bioavailability for Thieno[3,2-*d*]pyrimidine Derivatives

Compound	R1	R2	IC$_{50}$^{a} (μM)			In vitro metabolic stability (%)^b (mouse, human)	Oral Bioavailability (%)^c (mouse, rat)
			p110α	U87MG	A2780		
1	H	H	0.008	1.10	0.27	25, 32	ND
11	Me	H	0.006	0.99	0.28	64, ND	ND
12	H	Me	0.021	ND	ND	5, 51	ND
6	Me$_2$NCH$_2$	H	0.003	ND	0.11	32, 74	11, ND
7	(structure)	H	0.004	0.42	0.07	13, 57	ND
8	(structure)	H	0.010	1.01	0.16	85, 85	10, 2
9	(structure)	H	0.007	0.80	0.19	90, 90	7, 0

^{a} The values are averages of at least 2 separate determinations with typical variations of less than ±30%. ^{b} Percent remaining after 30 min incubation of 10 μM compound with 1 mg/mL mouse and human liver microsomes with both NADPH and UDPGA cofactors for glucuronidation. The values are averages of at least 2 separate determinations with typical variations of less than ±30%. ^{c} Based on iv and po administration (10 mg/kg). ND: Not determined (compound was not tested).

It was found that the 6-position was tolerant to a wide range of substituents with many analogues of various structural topologies displaying similar levels of biochemical activity to **1**. Among the more interesting compounds were tertiary amine derivatives such as compounds **6**–**9**, which offered the potential for facile salt formation to aid kinetic solubility, dissolution rates, as well as in vivo absorption and tumor exposure. Compounds **6**–**9** showed potent inhibition of p110α and good inhibition of cancer cell proliferation, and in addition, compounds **7**, **8**, and **9** demonstrated high solubility (>100 μM) as assessed in a turbidimetric aqueous solubility assay.[23]

Analysis of **1** docked into a homology model of p110α (Figure 2), which is based upon the crystal structure of p110γ,[24] suggested that groups located at the 6-position of the thiophene ring would extend out of the ATP-binding pocket toward solvent, thereby explaining the tolerance to a large variety of groups at this position. This model also indicated that the oxygen atom of the morpholine ring forms a hydrogen bond with the hinge Val851 (p110α numbering). Crystallographic studies of LY294002 with p110γ [24] have shown that the oxygen atom of the morpholine ring forms a key hydrogen bond with Val882 (p110γ numbering), supporting the hypothesis that the morpholine groups in both **1** and LY294002 bind in similar manner.

Encouragingly, compounds **8** and **9** also displayed enhanced metabolic stability in human and mouse liver microsomes relative to the other members of this series (Table 1). However, despite the encouraging microsomal stability, pharmacokinetic studies of several phenolic derivatives, including compounds **6**, **8**, and **9**, indicated very low oral bioavailability in mouse and rat, mainly as a result of glucuronidation. Following ip administration of compound **8** in mice, the circulating concentration of the glucuronide conjugate appeared greater than that of the parent phenol at all time points after 0.5 h (Figure 3), demonstrating the propensity for formation of glucuronide

Figure 3. Metabolism of **8** (mesylate salt) after ip dosing in female balb C mice at 50 mg/kg.

conjugates by the phenolic derivatives. In vitro metabolism studies in microsomes also indicated that glucuronidation of the parent compound was common to all the phenol derivatives (data not shown), suggesting that the phenolic group was a metabolic liability.

To overcome this liability, we explored isosteres for the phenolic group, which we hoped would provide the required level of activity without displaying the propensity for glucuronidation shown by the phenolic derivatives. We believed that a hydrogen bond donor was critical for activity as previous attempts to replace the 3-hydroxyphenyl group on related templates had resulted in a significant loss of activity.[18,19] Analysis of the structural model (Figure 2) suggested that the 3-hydroxyl group forms an interaction with Asp810 (p110α numbering) located at the back end of the ATP binding pocket of p110α, and consequently, we were particularly interested in investigating heterocyclic groups that maintained the potential

Table 2. Inhibition of p110α Activity and Cancer Cell Proliferation for Indazole Analogues

Compound	R	IC$_{50}$^{a} (µM)		
		p110α	U87MG	A2780
1	(structure, phenol)	0.008	1.10	0.27
20	(structure, indazole)	0.102	8.32	1.01
22	(structure, indazole)	2.45	ND	ND

^{a} The values are averages of at least 2 separate determinations with typical variations of less than ±30%. ND: Not determined (compound was not tested).

Table 3. Inhibition of p110α Activity, Cancer Cell Proliferation, and Metabolic Stability for Indazole Derivatives

Compound	R1	IC$_{50}$^{a} (µM)			In vitro metabolic stability (%)^b (mouse, human)
		p110α	U87MG	A2780	
16	(methylpiperazine)	0.044	7.88	1.40	81, 81
17	(sulfonylpiperazine)	0.003	0.95	0.14	91, 96

^{a} The values are averages of at least 2 separate determinations with typical variations of less than ±30%. ^{b} Percent remaining after 30 minutes incubation of 10 µM compound with 1 mg/mL mouse and human liver microsomes with both NADPH and UDPGA cofactors for glucuronidation. The values are averages of at least 2 separate determinations with typical variations of less than ±30%.

Table 4. Inhibition of Classes I, II, III, and IV PI3K Isoforms by **17**

enzyme	IC$_{50}$^{a} (µM)
p110α (class 1A)	0.003
p110α (class 1A) mutant E545-K	0.003
p110α (class 1A) mutant H1047-R	0.003
p110β (class 1A)	0.033
p110δ (class 1A)	0.003
p110γ (class 1B)	0.075
C2β (class II)	0.670
Vps34 (class III)	>10
DNA-PK (class IV)	1.23
mTOR (class IV)	0.58^b

^{a} The values are averages of at least 2 separate determinations with typical variations of less than ± 30%. ^{b} K_{iapp} value.
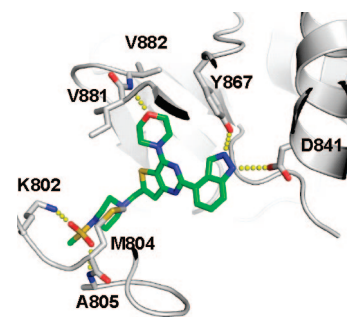
Figure 4. Crystal Structure of **17** bound to p110γ (p110γ numbering displayed).

istrations in the mouse indicated that a glucuronide conjugate was present but at significantly lower levels than the parent. Further optimization of **16** followed, in which functional groups were introduced that had the potential to form additional hydrogen bonds with residues located near the mouth of the ATP-binding pocket. Because of the biochemical and cellular potency of the functionalized piperazines and piperidines for the phenol-containing series, together with their potential for protonation to enhance solubility, we focused much of our attention on groups of this class. This led to the discovery of the sulfonylpiperazine derivative **17**, which showed a marked improvement in both biochemical and cellular potency compared to **16** (Table 3).

The crystal structure of **17** bound to p110γ (Figure 4) confirmed that the binding mode was largely as predicted from the in silico modeling and clarifies the high potency observed with compound **17**. The morpholine moiety of **17** is in close proximity to the hinge region of the kinase with the oxygen, forming a hydrogen bond to the amide of V882 and the carbon atoms packing against the side chain of I881. The hydrophobic thienopyrimidine core of the compound packs against the side chains of M804, W812, and I831 from the N-terminal lobe and the side chains from M953 and I963 from the C-terminal lobe of the kinase. The indazole moiety points toward a pocket formed by residues K833, D836, L838, Y867, and D964 with the two nitrogen atoms in H-hydrogen bonding distance to the phenol oxygen of Y867 and the carboxyl group of D841. Finally, the 4-methanesulfonyl-piperazin-1-ylmethyl group extends toward the solvent with the piperazine ring packing against the side chain of M804 and the oxygens of the sulfonyl group positioned in H-bonding distance with the side chain of K802 and the amide nitrogen of A805.

The pharmacokinetic properties of **17** were extensively studied. Acceptable oral bioavailability was achieved in all species tested, including mouse (77%), rat (30%), dog (71%), and monkey (20%). The pharmacokinetic profile in the dog, in which **17** had moderate clearance, is presented in Figure 5. On
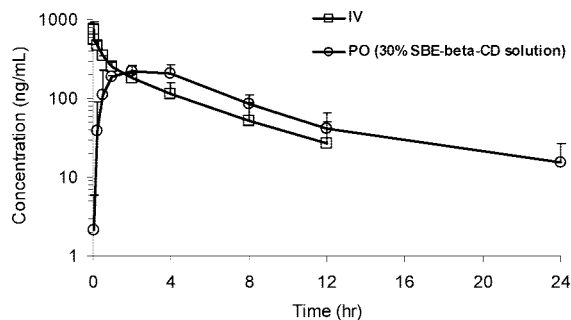
to act as a hydrogen bond donor. Homology model analysis also revealed that the phenol hydroxyl could potentially participate in hydrogen bonding with Tyr836 (p110α numbering), also located at the back end of the pocket. Indazoles were among the groups explored as replacements for phenols, and the 4-indazolyl derivative **20** showed encouraging biochemical activity, albeit 12-fold less potent than the corresponding phenol derivative **1** (Table 2). In contrast, the 6-indazolyl derivative **22** showed a 300-fold reduction in activity relative to **1**.

Introduction of the 4-methylpiperazin-1-ylmethylene group (Table 3), which had provided good solubility and improved metabolic stability in the phenolic series, resulted in **16**. This compound displayed modest potency and was metabolically stable in mouse and human microsomes. Encouragingly, compound **16** exhibited improved oral bioavailability in both rat (37%) and mouse (31%). Analysis of the peak areas of the metabolites of **16** in plasma following both iv and po admin-

Figure 5. Mean (±SD) plasma concentrations (average of three dogs dosed) of **17** (dimesylate salt) following a single administration iv (1 mg/kg) or po solution (2 mg/kg) of **17** to male beagle dogs. Pharmacokinetic parameters: Cl = 11.9 mL/min/kg; F = 71%; $t_{1/2}$ = 3.5 h; V_{ss} = 2.91 L/kg.

Table 5. Inhibition of Cancer Cell Proliferation and Signaling in Selected Cell Lines by **17**

cancer cell line	molecular features	proliferation IC$_{50}$[a] (μM)	pAkt^{473} IC$_{50}$ (μM)
U87MG (glioblastoma)	PTEN null	0.95	0.046[b]
PC3 (prostate)	PTEN null	0.28	0.037[c]
MDA-MB-361 (breast)	*PIK3CA* mutant E545-K	0.72	0.028[c]

[a] The values are averages of at least 2 separate determinations with typical variations of less than ± 30%. [b] Measured using Biosource ELISA. [c] Measured using MesoScale Discovery electrochemiluminescence ELISA.

the basis of good biochemical and cellular activity and pharmacokinetic properties, compound **17** was chosen for further evaluation.

The activity of **17** against the PI3K isoform family is presented in Table 4, which shows that the compound is equipotent against p110α and 110δ, while displaying modest levels of selectivity against p110β (10-fold) and p110γ (25-fold). However, greater levels of selectivity are observed for compound **17** when tested against members of PI3K classes II, III, and IV, including C2β, Vps34, DNA-PK, and mTOR. Compound **17** was also tested against two of the p110α mutant enzymes detected in human cancer. E545-K, which is a hotspot mutation in the helical domain and H1047-R, a hotspot mutation located in the C-terminal portion of the kinase domain, have both been shown to have elevated lipid kinase activity relative to the wild type and represent two of the three hotspots responsible for 80% of p110α mutations.[5,30,31] Compound **17** was found to be equipotent against both mutants when compared to the wild type protein (Table 4). Experiments have also indicated that **17** is a potent, ATP competitive inhibitor of p110α with a K_i value of 10.2 ± 4.4 nM (data not shown). Compound **17** displayed outstanding selectivity for the PIK family kinases over a panel of 228 kinases in the KinaseProfiler panel from Millipore (formerly Upstate Biotechnologies).[32] Of the 228 kinases tested, only two displayed greater than 50% inhibition by 1 μM **17**. The human tyrosine kinase Flt3 displayed 59% inhibition by the test article, and the human kinase TrkA displayed 61% inhibition by 1 μM **17**. The IC$_{50}$ value of **17** for inhibition of TrkA was subsequently determined to be 2.85 μM (data not shown). Thus, **17** demonstrates at least 300-fold selectivity for inhibition of p110α /p85α over other assayable kinases.

Compound **17** was tested using the 96 h Alamar Blue assay against a wider panel of human tumor cell lines, which included glioblastoma, breast, and prostate lines that have genetic aberrations in the PI3K pathway (Table 5). These data demonstrate that **17** is a potent inhibitor of cell proliferation in these
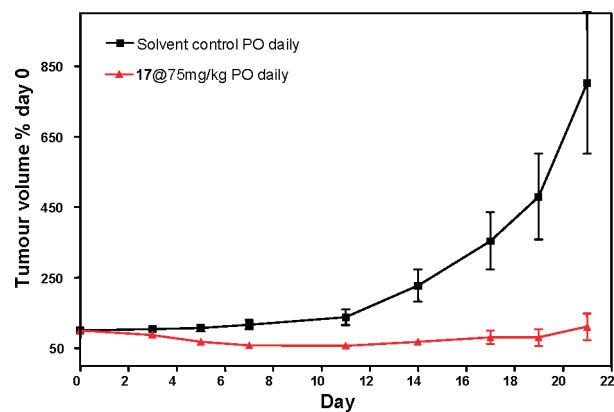

Figure 6. Growth inhibitory effect of **17** on established human U87MG glioblastoma xenografts in female NCr athymic mice (N = 12 per group, mean ± SD).

cell lines with submicromolar IC50s. The antiproliferative effects of the compound were associated with inhibition of intracellular PI3K pathway by measuring Akt (Ser473) phosphorylation. Potent inhibition of Akt (Ser473) phosphorylation was observed in U87MG, PC3, and MDA-MB-361 cells with IC$_{50}$s of 46, 37, and 28 nM, respectively.

Furthermore, **17** shows minimal inhibition of six of the principal cytochrome P450 isoforms,[33] and at a concentration of 25 μM, there is negligible induction of CYP1A and CYP3A4.[34] Also, there was no significant blockade of the hERG channel for this compound (IC$_{50}$ = 64 μM) in the patch clamp assay.[35]

17 was selected for in vivo efficacy studies in established U87MG human glioblastoma xenografts grown subcutaneously in female NCr athymic mice (Figure 6). When dosed orally at 75 mg/kg daily, tumor growth inhibition of 83% (based on weights of excised tumors compared to controls) was observed after 21 days with no body weight loss. A dose−response relationship was seen over the range 25−150 mg/kg/day. Evidence of target inhibition was provided by a decrease in p-Akt levels as measured in explanted xenograft tumors by electrochemiluminescence immunoassay. For example p-Akt levels fell to 5% of control values 30 min following an oral dose of 75 mg/kg and were undetectable at 1 and 4 h time points. Further details will be provided in a future publication.

Conclusion

A series of thieno[3,2-*d*]pyrimidine derivatives have been prepared and evaluated as inhibitors of PI3K. Structural modifications were targeted primarily at improving the pharmacokinetic properties of lead compound **1**. Replacement of the 3-hydroxyphenyl group with a 4-indazolyl group reduced the issue of glucuronidation and resulted in acceptable oral bioavailability. Further modifications led to the discovery of **17**, which has been extensively profiled and shown to be a potent and highly selective inhibitor of members of Class I PI3K. The compound shows potent growth inhibitory activity in vitro in a range of human tumor cell lines and exhibits a strong inhibitory effect on the growth of human U87MG glioblastoma xenografts in athymic mice. Compound **17** demonstrates an acceptable pharmaceutical profile and is currently being evaluated in human clinical trials for the treatment of cancer.

Experimental Section

Chemistry. All solvents and reagents were used as obtained. ¹H NMR spectra were recorded with a Bruker Avance DPX400

Spectrometer; chemical shifts are expressed as δ units using tetramethylsilane as the external standard (in NMR description, s, singlet; d, doublet; t, triplet; q, quartet; m, multiplet; and br, broad peak). Mass spectra were measured with a Finnigan SSQ710C spectrometer using an ESI source coupled to a Waters 600MS HPLC system operating in reverse mode with an X-bridge Phenyl column of dimensions 150 mm by 4.6 mm, with 5 μm sized particles.

4-morpholin-4-yl-2-[3-(1,1,2,2-tetramethyl-propylsilanyloxy)-phenyl]-thieno[3,2-d]pyrimidine (4). A mixture of **3**[22] (2.65 g, 10.37 mmol), 3-(*tert*-butyldimethylsilyloxy)phenyl boronic acid (3.40 g, 1.3 equiv), sodium bicarbonate (1.74 g, 2 equiv), PdCl$_2$(PPh$_3$)$_2$ (365 mg, 5%), DME (50 mL), and water (15 mL) was heated to reflux. After 16 h, the reaction mixture was cooled, diluted with ethyl acetate, washed with brine, dried (MgSO$_4$), and the solvent removed in vacuo. Purification on silica (EtOAC/hexanes, 1:4) yielded the desired compound (2.28 g, 51%). ^{1}H NMR (400 MHz, CDCl$_3$) δ 0.25 (s, 6H), 1.03 (s, 9H), 3.85−3.89 (m, 4H), 4.05−4.09 (m, 4H), 6.92−6.96 (m, 1H), 7.30−7.33 (m, 1H), 7.53 (d, J = 5.49 Hz, 1H), 7.76 (d, J = 5.46 Hz, 1H), 7.93 (s, 1H), 8.02−8.05 (m, 1H).

4-Morpholin-4-yl-2-[3-(1,1,2,2-tetramethyl-propylsilanyloxy)-phenyl]-thieno[3,2-d]pyrimidine-6-carbaldehyde(5). To a solution of **4** (2.26 g, 5.29 mmol) in dry THF (40 mL) cooled to −78 °C was added nBuLi (2.5 M solution in hexanes, 2.75 mL). After stirring for 20 min, dry *N,N*-dimethylformamide (617 μL, 1.5 equiv) was added, and the reaction mixture was stirred for 20 min at −78 °C and then warmed slowly to room temperature. After a further 30 min at room temperature, the reaction mixture was quenched with ice/brine and extracted exhaustively with chloroform. The combined organic extracts were dried (MgSO$_4$) and the solvent removed in vacuo to yield **5** as a yellow solid (2.38 g, 99%). ^{1}H NMR (400 MHz, CDCl$_3$) δ 0.24 (s, 6H), 1.01 (s, 9H), 3.89−3.92 (m, 4H), 4.11−4.14 (m, 4H), 6.92−6.96 (m, 1H), 7.32−7.36 (m, 1H), 7.92 (s, 1H), 8.02 (d, J = 7.70 Hz, 1H), 8.13 (s, 1H), 10.19 (s, 1H).

3-[6-(4-Methyl-piperazin-1-ylmethyl)-4-morpholin-4-yl-thieno[3,2-d]pyrimidin-2-yl]-phenol (8). A mixture of **5** (6.67 g, 14.66 mmol), *N*-methylpiperazine (2.11 mL, 1.3 equiv), and acetic acid (838 μL, 1.0 equiv) was stirred in 1,2-dichloroethane (70 mL) at room temperature. To this was added sodium triacetoxyborohydride (3.42 g, 1.1 equiv), and the reaction mixture was stirred for 3 days. The reaction mixture was then quenched with aqueous sodium bicarbonate solution, extracted exhaustively with chloroform, dried (MgSO$_4$), and the solvent removed in vacuo to yield a yellow oil. This was purified using flash chromatography (silica, ethyl acetate to ethyl acetate/methanol) to yield 6-(4-methyl-piperazin-1-ylmethyl)-4-morpholin-4-yl-2-[3-(1,1,2,2-tetramethyl-propylsilanyloxy)-phenyl]-thieno[3,2-d]pyrimidine (6.95 g, 88%). To a solution of 6-(4-methyl-piperazin-1-ylmethyl)-4-morpholin-4-yl-2-[3-(1,1,2,2-tetramethyl-propylsilanyloxy)-phenyl]-thieno[3,2-d]pyrimidine (6.95 g, 12.89 mmol) in THF (100 mL) cooled to 0 °C was added a 1.0 M solution of tetrabutyl ammonium fluoride in THF (14.2 mL, 1.1 equiv). After 30 min, the solvent was removed in vacuo and the residue was purified using flash chromatography (silica, 8% methanol in dichloromethane) and then triturated using ethyl acetate/methanol to yield **8** as a white solid (4.62 g, 85%). ^{1}H NMR (400 MHz, CDCl$_3$) δ 2.27 (s, 3H), 2.49 (sbr, 8H), 3.79 (s, 2H), 3.82−3.84 (m, 4H), 4.00−4.03 (m, 4H), 6.88−6.91 (m, 1H), 7.24−7.28 (m, 2H), 7.69−7.70 (m, 1H), 7.81 (d, J = 7.8 Hz, 1H). MS (ESI): m/z (M + H)$^+$ 426. Analytical LC-MS using Waters XBridge Phenyl analytical column and H20/MeCN modified with 0.1% formic acid running a linear gradient from 10% MeCN to 100% MeCN monitored by UV wavelength 210 nm and ESI+ TIC MS showed >99% purity.

3-(6-Dimethylaminomethyl-4-morpholin-4-yl-thieno[3,2-d]pyrimidin-2-yl)-phenol (6). Compound **6** was prepared from **5** according to the same procedure described for **8** using dimethylamine. ^{1}H NMR (400 MHz, CDCl$_3$) δ 2.39 (s, 6H), 3.74 (s, 2H), 3.82−3.86 (m, 4H), 4.01−4.04 (m, 4H), 5.70 (s, br, 1H), 6.90−6.92 (m, 1H), 7.31−7.35 (m, 2H), 7.89 (d, J = 2.4 Hz, 1H), 8.00 (d, J = 7.8 Hz, 1H). MS (ESI): m/z (M + H)$^+$ 371. Analytical LC-MS using Waters

XBridge Phenyl analytical column and H20/MeCN modified with 0.1% formic acid running a linear gradient from 10% MeCN to 100% MeCN monitored by UV wavelength 210 nm and ESI+ TIC MS showed 95.6% purity.

3-(6-{[(2-Methoxy-ethyl)-methyl-amino]-methyl}-4-morpholin-4-yl-thieno[3,2-d]pyrimidin-2-yl)-phenol (7). Compound **7** was prepared from **5** according to the same procedure described for **8**, using *N*-(2-methoxyethyl)methylamine. ^{1}H NMR (400 MHz, CDCl$_3$) δ 2.41 (s, 3H), 2.71 (t, J = 5.6 Hz, 2H), 3.38 (s, 3H), 3.56 (t, J = 5.6 Hz, 2H,), 3.84−3.88 (m, 4H), 3.90 (s, 2H), 4.03−4.07 (m, 4H), 6.92 (dd, 1H), 7.30 (s, 1H), 7.33 (t, J = 7.9 Hz, 1H), 7.92 (s, 1H), 7.99 (d, J = 7.8 Hz, 1H). MS (ESI): m/z (M + H)$^+$ 415. Analytical LC-MS using Waters XBridge Phenyl analytical column and H20/MeCN modified with 0.1% formic acid running a linear gradient from 10% CH3CN to 100% CH3CN monitored by UV wavelength 210 nm and ESI+ TIC MS showed 96.1% purity.

3-{6-[4-(2-Hydroxy-ethyl)-piperazin-1-ylmethyl]-4-morpholin-4-yl-thieno[3,2-d]pyrimidin-2-yl}-phenol (9). Compound **9** was prepared from **5** according to the same procedure described for **8** using 1-piperazine ethanol. ^{1}H NMR (400 MHz, CDCl$_3$) δ 2.63 (mbr, 10H), 3.65 (m, 2H), 3.84 (s, 2H), 3.87−3.90 (m, 4H), 4.04−4.06 (m, 4H), 6.93 (d, J = 10.0 Hz,1H), 7.32−7.36 (m, 2H), 7.91 (s, 1H), 8.01 (d, J = 7.74 Hz, 1H). MS (ESI): m/z (M + H)$^+$ 456. Analytical LC-MS using Waters XBridge Phenyl analytical column and H20/CH3CN modified with 0.1% formic acid running a linear gradient from 10%CH3CN to 100% CH3CN monitored by UV wavelength 210 nm and ESI+ TIC MS showed 99% purity.

2-Chloro-6-methyl-4-morpholin-4-yl-thieno[3,2-d]pyrimidine (10). To a suspension of **3**[22] (543 mg, 2.18 mmol) in dry THF cooled at −78 °C was added a 2.5 M solution of nBuLi in hexanes (1.02 mL, 1.2 equiv). After stirring for 1 h, methyl iodide (158 μL, 1.2 equiv) was added. The reaction mixture was stirred for 1 h at −78 °C and then warmed slowly to room temperature. After stirring for 2 days, the reaction mixture was poured onto ice/water and extracted into ethyl acetate. The organic phase was collected, dried (MgSO$_4$), and the solvent removed in vacuo to yield **10** as a beige solid (470 mg, 82%). ^{1}H NMR (400 MHz, DMSO-d_6) δ 2.62 (s, 3H), 3.78−3.81 (m, 4H), 3.86−3.90 (m, 4H), 7.18 (s, 1H).

3-(6-Methyl-4-morpholin-4-yl-thieno[3,2-d]pyrimidin-2-yl)-phenol (11). A mixture of **10** (252 mg, 0.93 mmol), 3-hydroxyphenyl boronic acid (141 mg, 1.1 equiv), sodium carbonate (235 mg, 3 equiv), PdCl$_2$(PPh$_3$)$_2$ (33 mg, 5%), DME (10 mL), and water (2 mL) was heated to reflux under argon. After 4 h, the reaction mixture was cooled, diluted with chloroform, washed with water, dried (MgSO$_4$), and the solvent removed in vacuo. Purification using column chromatography (EtOAc/hexanes to EtOAc) yielded the desired compound (30 mg, 10%). ^{1}H NMR (400 MHz, d_6-DMSO) δ 2.65 (s, 3H), 3.80−3.84 (m, 4H), 3.95−3.99 (m, 4H), 6.85−6.88 (m, 1H), 7.25−7.29 (m, 2H), 7.81−7.84 (m, 2H), 9.52 (s, 1H). MS (ESI): m/z (M + H)$^+$ 328.

2-Chloro-4-morpholin-4-yl-thieno[3,2-d]pyrimidine-6-carbaldehyde (13). To a suspension of **3**[22] (1.75 g, 6.85 mmol) in dry tetrahydrofuran (40 mL) at −78 °C was added a 2.5 M solution of nBuLi in hexanes (3.3 mL, 1.2 equiv). After stirring for 1 h, dry *N,N*-dimethylformamide (796 μL, 1.5 equiv) was added. The reaction mixture was stirred for 1 h at −78 °C and then warmed slowly to room temperature. After a further 2 h at room temperature, the reaction mixture poured onto ice/water, yielding a yellow precipitate. This was collected by filtration and air-dried to yield the title compound (1.50 g, 77%). ^{1}H NMR (400 MHz, DMSO-d_6) δ 3.74−3.78 (m, 4H), 3.94−3.97 (m, 4H), 8.28 (s, 1H), 10.20 (s, 1H).

2-Chloro-6-(4-methyl-piperazin-1-yl methyl)-4-morpholin-4-yl-thieno[3,2-d]pyrimidine (14). To a mixture of **13** (147 mg, 0.52 mmol), 1-methyl-piperazine (87 μL, 1.5 equiv) and acetic acid (32 μL, 1.05 equiv) in 1,2-dichloroethane (3 mL) was added sodium triacetoxyborohydride (121 mg, 1.1 equiv) and then stirred at room temperature overnight. The reaction mixture was diluted with dichloromethane, washed with a saturated solution of sodium hydrogen carbonate, brine, separated, and dried (MgSO$_4$). The crude product was evaporated in vacuo and purified by chromatography

to give **14** as an off-white crystalline solid (51 mg, 45%). ^{1}H NMR (400 MHz, CDCl$_3$) δ 2.21 (s, 3H), 2.40−2.55 (m, br, 8H), 3.72 (s, 2H), 3.75−3.79 (m, 4H), 3.93−3.96 (m, 4H), 7.11 (s, 1H).

2-Chloro-6-(4-methanesulfonyl-piperazin-1-ylmethyl)-4-morpholin-4-yl-thieno[3,2-*d*]pyrimidine (15). A mixture of **13** (5.56 g, 19.6 mmol), 1-methanesulfonyl-piperazine hydrochloride (4.72 g, 1.2 equiv), and trimethylorthoformate (6.42 mL, 3 equival) was stirred in 1,2-dichloroethane (100 mL) for 6 h at room temperature. To this was added sodium triacetoxyborohydride (10.39 g, 2.5 equiv), and the reaction mixture was stirred for 24 h at room temperature. The mixture was then quenched with brine, extracted with dichloromethane, dried (MgSO$_4$), and the solvent removed in vacuo. The residue was triturated with hot ethyl acetate to yield **15** as a white solid (1.01 g). NMR ^{1}H NMR (400 MHz, CDCl$_3$) δ 2.69−2.71 (m, 4H), 2.79 (s, 3H), 3.30−3.33 (m, 4H), 3.82−3.86 (m, 6H), 3.98−4.01 (m, 4H), 7.18 (s, 1H).

2-(1*H*-Indazol-4-yl)-6-(4-methyl-piperazin-1-ylmethyl)-4-morpholin-4-yl-thieno[3,2-*d*]pyrimidine (16). Compound **16** was prepared from **14** according to the same procedure described for **17**. ^{1}H NMR (400 MHz, DMSO-d_6) δ 2.18 (s, 3H), 2.30−2.45 (m, 4H), 2.48−2.55 (m, 4H), 3.82−3.84 (m, 4H), 3.86 (s, 2H), 3.98−4.00 (m, 4H), 7.44−7.47 (m, 2H), 7.65 (d, J = 8.2 Hz, 1H), 8.21 (d, J = 7.2 Hz, 1H), 8.87 (s, 1H), 13.16 (s, br,1H). MS (ESI): *m/z* (M + H)$^+$ 450. Analytical LC-MS using Waters XBridge Phenyl analytical column and H20/MeCN modified with 0.1% formic acid running a linear gradient from 10% MeCN to 100% MeCN monitored by UV wavelength 210 nm and ESI+ TIC MS showed 98.4% purity.

2-(1*H*-Indazol-4-yl)-6-(4-methanesulfonyl-piperazin-1-ylmethyl)-4-morpholin-4-yl-thieno[3,2-*d*]pyrimidine (17). A mixture of **15** (2.00 g, 4.63 mmol), **25** (2.26 g, 2 equiv), toluene (24 mL), ethanol (12 mL), water (6 mL), sodium carbonate (1.72 g, 3.5 equiv), and PdCl$_2$(PPh$_3$)$_2$ (325 mg, 0.1 equiv) was heated to 130 °C in the microwave for 90 min. The reaction mixture was cooled, diluted with chloroform, washed with brine, dried (MgSO$_4$), and the solvent removed in vacuo. The residue was purified using flash chromatography (chloroform to 10% methanol/chloroform) and then trituration with ether, yielding the desired title compound as a white solid (1.42 g, 60%). ^{1}H NMR (CDCl$_3$) δ 2.67−2.71 (m, 4H), 2.81 (s, 3H), 3.29−3.33 (m, 4H), 3.89 (s, 2H), 3.89−3.93 (m, 4H), 4.08−4.12 (m, 4H), 7.41 (s, 1H), 7.51 (t, J = 7.2 Hz, 1H), 7.60 (d, J = 8.3 Hz, 1H), 8.28 (d, J = 7.5 Hz, 1H), 9.02 (s, 1H), 10.10 (s, br,1H). MS (ESI): *m/z* (M + H)$^+$ 514. Anal. (C$_{23}$H$_{27}$N$_7$O$_3$S$_2$) C, H, N. Analytical LC-MS using Waters XBridge Phenyl analytical column and H20/MeCN modified with 0.1% formic acid running a linear gradient from 10% MeCN to 100% MeCN monitored by UV wavelength 210 nm and ESI+ TIC MS showed 98% purity.

2-Methyl-3-(4,4,5,5-tetramethyl-[1,3,2]dioxaborolan-2-yl)-phenylamine (18). To a solution of 3-bromo-2-methylaniline (1.00 g, 5.38 mmol) in dioxane (15 mL) was added triethylamine (3.0 mL, 4 equiv), Pd(OAc)$_2$ (60 mg, 5%), 2-dicyclohexylphosphinobiphenyl (377 mg, 20%), and pinacol borane (2.34 mL, 3 equiv), and the reaction mixture was heated to 80 °C for 1 h. The reaction mixture was then cooled, diluted with ethyl acetate, washed with brine, dried (MgSO$_4$), and the solvent reduced in vacuo. The residue was purified using flash chromatography (EtOAc/hexane 1:4) to yield **18** as a brown oil (1.07 g, 85%). ^{1}H NMR (400 MHz, CDCl$_3$) δ 1.27 (s, 12H), 2.31 (s, 3H), 3.52 (s, 2H), 6.68 (d, J = 7.8 Hz, 1H), 6.92−6.96 (m, 1H), 7.14 (d, J = 7.4 Hz, 1H)

2-Methyl-3-(4-morpholin-4-yl-thieno[3,2-*d*]pyrimidin-2-yl)-phenylamine (19). A mixture of **3** (169 mg, 0.66 mmol), **18** (155 mg, 0.66 mmol), sodium carbonate (140 mg, 2 equiv), DME (10 mL), water (3 mL), and PdCl$_2$(PPh$_3$)$_2$ (23 mg, 5%) was heated to reflux. After 16 h, the reaction mixture was cooled, diluted with ethyl acetate, washed with brine, dried (MgSO$_4$), and reduced in vacuo. The residue was purified using flash chromatography (EtOAc/hexanes 1:1 to EtOAc) to yield **19** (148 mg, 69%). ^{1}H NMR (400 MHz, CDCl$_3$) δ 2.29 (s, 3H), 3.70 (s, br, 2H), 3.85−3.88 (m, 4H), 4.01−4.06 (m, 4H), 6.73−6.76 (m, 1H), 7.08−7.13 (m, 2H), 7.51 (d, J = 5.5 Hz, 1H), 7.77 (d, J = 5.5 Hz, 1H).

2-(1*H*-Indazol-4-yl)-4-morpholin-4-yl-thieno[3,2-*d*]pyrimidine (20). To a solution of **19** (80 mg, 0.25 mmol) in chloroform (8 mL) and acetic acid (4 mL) was added isoamyl nitrite (36 μL, 1.1 equiv). The reaction mixture was stirred for 1 day at room temperature. The mixture was then quenched with sodium bicarbonate solution and extracted in to chloroform and reduced in vacuo. The residue was purified using flash chromatography (EtOAC/hexanes to EtOAc) to yield **20** (17 mg, 20%). ^{1}H NMR (400 MHz, DMSO-d_6) δ 3.86−3.91 (m, 4H), 4.05−4.09 (m, 4H), 7.48−7.52 (m, 1H), 7.63−7.70 (m, 2H), 8.26 (d, 1H), 8.33 (d, 1H), 8.95 (s, 1H), 13.20 (s, br, 1H). MS (ESI): *m/z* (M + H)$^+$ 338. Analytical LC-MS using Waters XBridge Phenyl analytical column and H20/MeCN modified with 0.1% formic acid running a linear gradient from 10% MeCN to 100% MeCN monitored by UV wavelength 210 nm and ESI+ TIC MS showed 98.2% purity.

2-(1*H*-Indazol-6-yl)-4-morpholin-4-yl-thieno[3,2-*d*]pyrimidine (22). A mixture of **3** (806 mg, 3.15 mmol), 3-amino-4-methylbenzeneboronic acid (524 mg, 1.1 equiv), DME (10 mL), water (5 mL), sodium carbonate (640 mg, 2 equiv), and PdCl$_2$(PPh$_3$)$_2$ (100 mg, 5%) was heated to reflux for 16 h. The reaction mixture was then cooled, diluted with ethyl acetate, and reduced in vacuo. The residue was purified using flash chromatography to yield 2-methyl-5-(4-morpholin-4-yl-thieno[3,2-*d*]pyrimidin-2-yl)-phenylamine (**21**) (840 mg, 82%). To a solution of **21** (99 mg, 0.30 mmol) in chloroform (10 mL) and acetic acid (2 mL) was added isoamyl nitrite (44 μL, 1.1 equiv). The reaction mixture was stirred for 2 days at room temperature. The mixture was then quenched with sodium bicarbonate solution and extracted into chloroform and reduced in vacuo. The residue was purified using flash chromatography (EtOAc) to yield the title compound (14 mg, 14%). ^{1}H NMR (400 MHz, DMSO-d_6) δ 3.85−3.89 (m, 4H), 4.05−4.09 (m, 4H), 7.58 (d, J = 5.4 Hz, 1H), 7.86 (d, J = 8.4 Hz, 1H), 8.12 (s, 1H), 8.12 (d, J = 8.5 Hz, 1H), 8.19 (d, J = 5.4 Hz, 1H), 8.21 (s, 1H), 13.22 (s, br, 1H). MS (ESI): *m/z* (M + H)$^+$ 338. Analytical LC-MS using Waters XBridge Phenyl analytical column and H20/MeCN modified with 0.1% formic acid running a linear gradient from 10% MeCN to 100% MeCN monitored by UV wavelength 210 nm and ESI+ TIC MS showed 95.5% purity.

4-Bromo-1*H*-indazole (24). To a solution of 3-bromo-2-methylaniline (5.00 g, 26.9 mmol) in chloroform (50 mL) was added potassium acetate (2.77 g, 28.2 mmol). Acetic anhydride (5.07 mL, 53.7 mmol) was added with concurrent cooling in ice−water. The mixture was then stirred at room temperature for 10 min, after which time a white gelatinous solid formed. 18-crown-6 (1.42 g, 5.37 mmol) was then added, followed by isoamyl nitrite (7.94 mL, 59.1 mmol), and the mixture was heated under reflux for 18 h. The reaction mixture was allowed to cool and was partitioned between chloroform and saturated aqueous sodium hydrogen carbonate. The combined organic extracts were washed with brine, separated, and dried (MgSO$_4$). The crude product was evaporated onto silica and purified by chromatography eluting with 20% to 40% EtOAc-petrol to provide 1-(4-bromo-indazol-1-yl)-ethanone **23** (3.14 g, 49%) and 4-bromo-1*H*-indazole **24** (2.13 g, 40%). To a solution of **23** (3.09 g, 12.9 mmol) in methanol (50 mL) was added 6M aqueous HCl (30 mL), and the mixture was stirred at room temperature for 7 h. The methanol was evaporated and the mixture partitioned between ethyl acetate and water. The combined organic layers were washed with brine, separated, and dried (MgSO$_4$). The solvent was removed by evaporation under reduced pressure to give **24** (2.36 g, 93%). ^{1}H NMR (400 MHz, CDCl$_3$) δ 7.25 (t, J = 7.3 Hz, 1H), 7.33 (d, J = 7.3 Hz, 1H), 7.46 (d, J = 7.3 Hz, 1H), 8.11 (s, 1H), 10.20 (s, br,1H).

4-(4,4,5,5-Tetramethyl-[1,3,2]dioxaborolan-2-yl)-1H-indazole (25). To a solution of **24** (500 mg, 2.54 mmol) and bis(pinacolato)diboron (967 mg, 3.81 mmol) in DMSO (20 mL) was added potassium acetate (747 mg, 7.61 mmol) and PdCl$_2$(dppf)$_2$ (62 mg, 0.076 mmol, 3 mol%). The mixture was degassed with argon and heated at 80 °C for 40 h. The reaction mixture was allowed to cool and partitioned between water and ether. The combined organic layers were washed with brine, separated, and dried (MgSO$_4$). The crude material was purified by chromatography eluting with 30% to 40%

EtOAc-petrol to give an inseparable 3:1 mixture of the desired product **25** (369 mg, 60%) and indazole (60 mg, 20%). ^{1}H NMR (400 MHz, DMSO-d_6) δ 1.41 (s, 12H), 7.40 (dd, $J = 8.4$ Hz, 6.9 Hz, 1H), 7.59 (d, $J = 8.4$ Hz, 1H), 7.67 (d, $J = 6.9$ Hz, 1H), 8.45 (s, 1H), 10.00 (s, br,1H).

Assays

Scintillation Proximity Assay. Recombinant human p110 α, β, and δ were coexpressed in an *Sf*9 baculovirus system with the p85α regulatory subunit and purified as GST-fusion proteins using affinity chromatography on glutathione-sepharose. Recombinant human p110γ, Vps34, and C2β proteins were expressed as monomeric GST-fusions and purified similarly. Test compounds were dissolved in DMSO and added to 20 mM Tris-HCl (pH 7.5) containing 200 μg yttrium silicate (Ysi) polylysine SPA beads (Amersham), 4 mM MgCl$_2$, 1 mM dithiothreitol (DTT), 1 μM ATP, and 0.125 μCi [γ-^{33}P]-ATP (Perkin-Elmer)), 4% (v/v) DMSO in a total volume of 50 μL. The recombinant GST-fusion of p110α/p85α (5 ng), p110β/p85α (5 ng), p110δ/p85α (5 ng), p110γ (5 ng), p110α/p85α(H1047-R)(5ng), p110α/p85α(E545-K) (5 ng), Vps 34 (40 ng), or C2β (5 ng) was added to the assay mixture to initiate the kinase reaction. After incubation for 1 h at room temperature, the kinase reaction was terminated with 150 μL PBS. The mixture was then centrifuged for 2 min at 2000 rpm and read using a Wallac Microbeta counter (Perkin-Elmer). The reported IC$_{50}$ values are means of at least 2 independent experiments and are calculated using a sigmoidal, dose−response curve fit (4 parameter logistic model [$y = A + ((B - A)/(1 + ((C/x)^D)]$) in MDL Assay Explorer.

mTOR assay. Mammalian target of rapamycin (mTOR) was assayed by monitoring phosphorylation of GFP-4EBP using a homogeneous time-resolved fluorescence resonance energy transfer format and assay reagents from Invitrogen. In the presence of 8 uM ATP, 50 mM Hepes (pH 7.5), 0.01% (v/v) Tween 20, 10 mM MnCl$_2$, 1 mM EGTA, and 1 mM DTT, the mTOR-mediated phosphorylation of 400 nM GFP-4E-BP1 was measured under initial rate conditions. After incubation at 25 °C for 30 min, the reaction was terminated by addition of 10 mM EDTA, and phosphorylated GFP-4E-BP1 was detected with 2 nM Tb-anti-p4E-BP1 antibody before reading on a Perkin-Elmer EnVision Fluorescence Reader (exc 340; em 495/520). Duplicate dose−response curves were fit to an equation of competitive tight-binding inhibition.

Proliferation Assay. The human tumor cell lines used were obtained from the ATCC. Cells were plated at 4 × 10^4 cells/mL and cultured at 37 °C with 5% CO$_2$ in DMEM supplemented with 10% fetal calf serum, and L-glutamine. Test compound was added to replicate wells in a volume of 10 μL such that the final DMSO concentration did not exceed 0.2%. After 4 days of incubation, 10 μL of Alamar Blue reagent was added and developed for 6 h at 37 °C before measuring the fluorescence excitation/emission (wavelength 540/595 nm) using a Victor plate reader. The reported IC$_{50}$ values are means of at least two independent experiments with variations of less than 20%.

p-Akt Assay. The human tumor cell lines used were obtained from the ATCC. Cells were plated in 6-well tissue culture plates in DMEM/RPMI1640 supplemented with 10% FCS and 2 mM L-glutamine. Test compound was added to replicate wells in a volume so that the final DMSO concentration did not exceed 0.2%. After 2 h incubation at 37 °C with 5% CO$_2$, cells were lysed at 4 °C and lysates centrifuged for 15 min at 14000 rpm. Protein concentration was established using the Pierce BCA protein assay kit (no. 23225). Assessment of p-AKT (S473) was carried out using either the BioSource p-AKT (Ser473) ELISA kit (no. KHO0111) and total Akt kit (no. KHO0101) with absorbance at 450 nm read on a Wallac Victor2 plate reader or the Meso Scale Discovery (MSD) MS6000 Phospho (Ser473)/ Total Akt Whole Cell Lysate Kit (no. K11100D-1) reading ECL signal using the MSD SECTOR Imager 6000 reader. Both assays were carried out according to the manufacturer's protocol. The reported IC$_{50}$ values are means of at least two independent experiments with variations of less than 20%.

Metabolic Stability Studies. Male CD1 mouse liver microsomes and mixed gender pooled human liver microsomes were purchased from Tebu-bio (Peterborough, U.K.). Incubations contained final concentrations of 1 mg/mL microsomal protein, 10 μmol/L test compound, 3 mmol/L MgCl$_2$, 1 mmol/L NADPH, 2.5 mmol/L UDP-glucuronic acid, and 10 mmol/L phosphate buffer (pH 7.4) (all purchased from Sigma Aldrich, Gillingham, U.K.) in a total volume of 200 μL and were performed for 0, 15, and 30 min at 37 °C. The reaction was terminated by the addition of 3 volumes of ice-cold methanol containing olomoucine (Sigma Aldrich, Gillingham, U.K.) as an internal standard. Samples were centrifuged at 2800g for 20 min at 4 °C and the supernatants analyzed. Control incubations were prepared as above but by omission of either cofactors or microsomes.

Pharmacokinetic Studies. Mouse studies. The mesylate salt of the appropriate compound was used in the study. Three male CD1 mice, 25−30 g, were dosed per administration route, per time point, per compound. The compounds were administered orally (via gavage) and iv (via the tail vein) at a dose level of 10 mg/kg per compound. Animals were given free access to food throughout the studies. At the appropriate times, the animals were anaesthetized and sacrificed and blood samples were collected and placed in heparinized tubes. Blood samples were taken at 0.08, 0.25, 0.5, 1, 2, 4, and 8 h following oral dosing and at 0.08, 0.25, 0.5, 1, 2, 4, and 8 h following intravenous dosing. Blood samples were centrifuged to obtain the plasma, which was aspirated into a separate labeled container. Aliquots from the three animals at each time point, for each route, were pooled. Standard curves were prepared in blank plasma matrices. Standards and samples from plasma were analyzed using a 3.5 min LC method. Parent compounds were quantified using specific MRM transition.

Pharmacokinetic Studies. Dog Study. The dimesylate salt of **17** was used for the study. Dosing formulations were prepared in 30% sulfobutylether-β-cyclodextrin (SBE-β-CD). Prepared dosing formulations were stored at 2−8 °C for up to 1 h before dosing. Three male purebred beagle dogs (Harlan Bioproducts for Science, Madison, WI) were used in this study. At the initiation of the study, dogs weighed from 12.8 to 14.1 kg. Only animals that appeared to be healthy and that were free of obvious abnormalities were used for the study.

This cross-over study was composed of two phases. In the first phase, 3 male dogs were given a single iv dose of 1 mg/kg of **17** via a cephalic vein. In the second phase, the same dogs were given po doses of 2 mg/kg of **17** in an SBE-β-CD solution. The two phases were each separated by a 7-day washout period. Animals were not fasted before dosing in the first of these phases, but they were fasted overnight before the second of these phases until 4 h postdose. Blood samples were collected from all animals after the first phase at predose and at 0.0033, 0.083, 0.25, 0.5, 1, 2, 4, 8, 12, and 24 h after the intravenous dose. Blood samples were collected from all animals in the second phase at predose and at 0.083, 0.25, 0.5, 1, 2, 4, 8, 12, and 24 h after the oral dose. The samples (approximately 3 mL per

sample) were collected from the jugular vein into tubes containing dipotassium ethylenediaminetetraacetic acid (K$_2$EDTA) as an anticoagulant. Blood samples were kept on ice and centrifuged for 10−15 min at 2000g and 2−8 °C within 1 h of collection. Plasma was collected and stored frozen at −60 °C to −80 °C until ready for analysis. The concentration (expressed as free base equivalents) of **17** in each plasma sample was determined by nonvalidated liquid chromatography-tandem mass spectrometry assays. The assay lower limit of quantitation (LLOQ) was 2.57 ng/mL for **17** in plasma. Concentrations of **17** in plasma were used to construct semilogarithmic plasma concentration−time curves for analysis. Pharmacokinetic parameters were determined by noncompartmental methods using WinNonlin version 5.1.1. (Pharsight Corporation, Mountain View, CA)

In Vivo Tumor Efficacy Study. Human tumor xenografts of U87MG glioblastoma were established in the bilateral flanks of female NCr athymic mice ($N = 12$ per group) from the inoculation of 2 million cells. All procedures involving animals were performed in accordance with National Home Office regulations under the Animals (Scientific Procedures) Act 1986 and within guidelines set out by the Institute's Animal Ethics Committee and the United Kingdom Coordinating Committee for Cancer Research's ad hoc Committee on the Welfare of Animals in Experimental Neoplasia.[36] Oral dosing with **17** commenced when tumors were well-established (∼5 mm diameter). Compound was dissolved in 10% DMSO, 5% Tween 20, 85% water, and administered orally at 75 mg/kg once daily by gavage. Mouse body weights were monitored throughout the study. Tumours were measured three times weekly across two perpendicular diameters and volumes calculated using the formula $V = {}^4/_3\pi[(d1 + d2)/4]^3$.[37] At the end of the study, tumors were excised, weighed, and the degree of growth inhibition calculated.

Crystallography studies. For structural studies, PI3Kγ was expressed, purified, and crystallized as described previously.[24] Crystals were soaked with compound and frozen in liquid nitrogen using established protocols.[24] Data to 2.7 Å resolution were collected at ALS beamline 5.0.2 to 2.8 Å; the structure was solved using molecular replacement and the coordinates of 1E8Y and refined to R/R_{free} of 21.9/26.2% with good stereochemistry.

References

(1) Vanhaesebroeck, B.; Leevers, S. J.; Ahmadi, K.; Timms, J.; Katso, R.; Driscoll, P. C.; Woscholski, R.; Parker, P. J.; Waterfield, M. D. Synthesis and function of 3-phosphorylated inositol lipids. *Annu. Rev. Biochem.* **2001**, *70*, 535–602.

(2) Cantley, L. C. The phosphoinositide 3-kinase pathway. *Science* **2002**, *296*, 1655–1657.

(3) Vivanco, I.; Sawyers, C. L. The phosphatidylinositol 3-kinase AKT pathway in human cancer. *Nat. Rev. Cancer* **2002**, *2*, 489–501.

(4) Shayesteh, L.; Kuo, W. L.; Baldocchi, R.; Godfrey, T.; Collins, C.; Pinkel, D.; Powell, B.; Mills, G. B.; Gray, J. W. PIK3CA is implicated as an oncogene in ovarian cancer. *Nat. Genet.* **1999**, *21*, 99–102.

(5) Samuels, Y.; Wang, Z.; Bardelli, A.; Silliman, N.; Ptak, J.; Szabo, S.; Yan, H.; Gazdar, A.; Powell, S. M.; Riggins, G. J.; Willson, J. K.; Markowitz, S.; Kinzler, K. W.; Vogelstein, B.; Velculescu, V. E. High frequency of mutations of the PIK3CA gene in human cancers. *Science* **2004**, *30*, 554.

(6) Parsons, D. W.; Wang, T. L.; Samuels, Y.; Bardelli, A.; Cummins, J. M.; DeLong, L.; Silliman, N.; Ptak, J.; Szabo, S.; Willson, J. K.; Markowitz, S.; Kinzler, K. W.; Vogelstein, B.; Lengauer, C.; Velculescu, V. E. Colorectal cancer: mutations in a signalling pathway. *Nature* **2005**, *436*, 792.

(7) Hennessy, B. T.; Smith, D. L.; Ram, P. T.; Lu, Y.; Mills, G. B. Exploiting the PI3K/AKT pathway for cancer drug discovery. *Nat. Rev. Drug Discovery* **2005**, *4*, 98–104.

(8) Sulis, M. L.; Parsons, R. PTEN: from pathology to biology. *Trends Cell. Biol.* **2003**, *13*, 478–483.

(9) Li, J.; Yen, C.; Liaw, D.; Podsypanina, K.; Bose, S.; Wang, S. I.; Puc, J.; Miliaresis, C.; Rodgers, L.; McCombie, R.; Bigner, S. H.; Giovanella, B. C.; Ittmann, M.; Tycko, B.; Hibshoosh, H.; Wigler, M. H.; Parsons, R. PTEN, a putative protein tyrosine phosphatase gene mutated in human brain, breast, and prostate cancer. *Science* **1997**, *275*, 1943–1947.

(10) She, Q. B.; Solit, D.; Basso, A.; Moasser, M. M. Resistance to gefitinib in PTEN-null HER-overexpressing tumor cells can be overcome through restoration of PTEN function or pharmacologic modulation of constitutive phosphatidylinositol 3′-kinase/Akt pathway signaling. *Clin. Cancer Res.* **2003**, *9*, 4340–4346.

(11) Berns, K.; Horlings, H. M.; Hennessy, B. T.; Madiredjo, M.; Hijmans, E. M.; Beelen, K.; Linn, S. C.; Gonzalez-Angulo, A. M.; Stemke-Hale, K.; Hauptmann, M.; Beijersbergen, R. L.; Mills, G. B.; van de Vijver, M. J.; Bernards, R. A functional genetic approach identifies the PI3K pathway as a major determinant of trastuzumab resistance in breast cancer. *Cancer Cell* **2007**, *12*, 395–402.

(12) Nagata, Y.; Lan, K. H.; Zhou, X.; Tan, M.; Esteva, F. J.; Sahin, A. A.; Klos, K. S.; Li, P.; Monia, B. P.; Nguyen, N. T.; Hortobagyi, G. N.; Hung, M. C.; Yu, D. PTEN activation contributes to tumor inhibition by trastuzumab, and loss of PTEN predicts trastuzumab resistance in patients. *Cancer Cell* **2004**, *6*, 117–127.

(13) Wee, S.; Lengauer, C.; Wiederschain, D. Class IA phosphoinositide 3-kinase isoforms and human tumorigenesis: implications for cancer drug discovery and development. *Curr. Opin. Oncol.* **2008**, *20*, 77–82.

(14) Drees, B. E.; Mills, G. B.; Rommel, C.; Prestwich, G. D. Therapeutic potential of phosphoinositide 3-kinase inhibitors. *Expert Opin. Ther. Patents* **2004**, *14*, 703–732.

(15) Schultz, R. M.; Merriman, R. L.; Andis, S. L.; Bonjouklian, R.; Grindley, G. B.; Rutherford, P. G.; Gallegos, A.; Massey, K.; Powis, G. In vitro and in vivo antitumor activity of the phosphatidylinositol-3-kinase inhibitor, wortmannin. *Anticancer Res.* **1995**, *15*, 1135–1139.

(16) Norman, B. H.; Shih, C.; Toth, J. E.; Ray, J. E.; Dodge, J. A.; Johnson, D. W.; Rutherford, P. G.; Schultz, R. M.; Worzalla, J. F.; Vlahos, C. J. Studies on the mechanism of phosphatidylinositol 3-kinase inhibition by wortmannin and related analogs. *J. Med. Chem.* **1996**, *39*, 1106–1111.

(17) Vlahos, C. J.; Matter, W. F.; Hui, K. Y.; Brown, R. F. A specific inhibitor of phosphatidylinositol 3-kinase, 2-(4-morpholinyl)-8-phenyl-4H-1-benzopyran-4-one (LY294002). *J. Biol. Chem.* **1994**, *269*, 5241–5248.

(18) Hayakawa, M.; Kaizawa, H.; Moritomo, H.; Koizumi, T.; Ohishi, T.; Okada, M.; Ohta, M.; Tsukamoto, S.; Parker, P.; Workman, P.; Waterfield, M. Synthesis and biological evaluation of 4-morpholino-2-phenylquinazolines and related derivatives as novel PI3 kinase p110α inhibitors. *Biorg. Med. Chem.* **2006**, *14*, 6847–6858.

(19) Hayakawa, M.; Kaizawa, H.; Moritomo, H.; Koizumi, T.; Ohishi, T.; Yamano, M.; Okada, M.; Ohta, M.; Tsukamoto, S.; Raynaud, F.; Workman, P.; Waterfield, M.; Parker, P. Synthesis and biological evaluation of pyrido[3′,2′:4,5]furo[3,2-d]pyrimidine derivatives as

novel PI3 kinase p110α inhibitors. *Biorg. Med. Chem. Lett.* **2007**, *17*, 2438–2442.

(20) Raynaud, F.; Eccles, S.; Clarke, P.; Hayes, A.; Nutley, B.; Alix, S.; Henley, A.; Di-Stefano, F.; Ahmad, Z.; Guillard, S.; Bjerke, L.; Kelland, L.; Valenti, M.; Patterson, L.; Gowan, S.; de Haven Brandon, A.; Hayakawa, M.; Kaizawa, H.; Koizumi, T.; Ohishi, T.; Patel, S.; Saghir, N.; Parker, P.; Waterfield, M.; Workman, P. Pharmacological Characterization of a Potent Inhibitor of Class I Phosphatidylinositide 3-Kinases. *Cancer Res.* **2007**, *67*, 5840–5850.

(21) Fan, Q. W.; Knight, Z. A.; Goldenberg, D. D.; Yu, W.; Mostov, K. E.; Stokoe, D.; Shokat, K. M.; Weiss, W. A. A dual PI3 kinase/mTOR inhibitor reveals emergent efficacy in glioblastoma. *Cancer Cell* **2006**, *9*, 341–349.

(22) Woitun, E.; Ohnacker, G.; Narr, B.; Horch, U.; Kadatz, R. U.S. Patent 3763156, 1973.

(23) Turbidimetric (kinetic) solubility measurements were conducted at Cyprotex using the Cloe screen. Measurements were made at pH 7.4 using 10 mM of compound in DMSO as the initial stock solution.

(24) Walker, E. H.; Pacold, M. E.; Perisic, O.; Stephens, L.; Hawkins, P. T.; Wymann, M. P.; Williams, R. L. Structural Determinants of Phosphoinoside 3-Kinase Inhibition by Wortmannin, LY294002, Quercetin, Myricetin, and Staurosporine. *Mol. Cell* **2000**, *6*, 909–919.

(25) Pirola, L.; Zvelebil, M. J.; Bulgarelli-Leva, G.; Van Obberghen, E.; Waterfield, M. D.; Wymann, M. P. Activation loop sequences confer substrate specificity to phosphoinositide 3-kinase alpha (PI3Kalpha). Functions of lipid kinase-deficient PI3Kalpha in signaling. *J. Biol. Chem.* **2001**, *276*, 21544.

(26) Zvelebil, M. J.; Baum, J. O. In *Understanding Bioinformatics*; Garland Publishing Inc.: New York, 2007.

(27) The three-dimensional model of p110α was created based upon the crystal structure of p110γ.[24] For docking purposes, only the catalytic domain of the protein was utilized, corresponding to residues 725 through 1092 based on p110γ sequence nomenclature, and the model was constructed as outlined previously.[25] For docking, we used the application DS Modelling 1.2 from Accelrys Ltd. Compound **1** was docked into the homology model to optimize shape complementarity and protein−ligand interactions. Initially, three force fields were employed: Dreiding (using Gasteiger charges), CFF, and PLP1 with a grid extension of 3.0Å, a non-bonded cut-off distance of 7.0Å, and a distance-dependent dielectric constant. A flexible fit, with a variable number of Monte Carlo trials, was conducted for each compound. Several scoring functions were employed used to calculate a score for each fit, namely Ligscore2, PLP1, PLP2, Jain, PMF, and a consensus score. To establish the most accurate docking procedure, we investigated the Dreiding, PLP1, and cff forcefields using the crystal structures of p110γ with ATP, Wortmannin, LY294002, Quercetin, Myricetin, and Staurosporine.[24,29] The structures of the docked compounds were compared to those determined from soaking studies,[24,29] and we concluded that the cff forcefield, in general, provided the best binding orientations. The definition of the binding site was a crucial step, and while in our docking analyses, we mainly employed the cff forcefield, and the number of highest scores along with the consensus score was used as a guide to an optimum ligand fit.

(28) Parts b and c of Figure 2 were generated using PyMOL, see: DeLano, W. L. *The PyMOL Molecular Graphics System*. DeLano Scientific: San Carlos, CA, 2002.

(29) Walker, E. H.; Perisic, O.; Reid, C.; Stephens, L.; Williams, R. L. *Nature* **1999**, *402*, 313.

(30) Samuels, Y.; Diaz, L. A.; Schmidt-Kittler, O.; Cummins, J. M.; DeLong, L.; Cheong, I.; Rago, C.; Huso, D. L.; Lengauer, C.; Kinzler, K. W.; Vogelstein, B.; Velculescu, V. E. Mutant PIK3CA promotes cell growth and invasion of human cancer cells. *Cancer Cell* **2005**, *7*, 561–573.

(31) Kang, S.; Bader, A. G.; Vogt, P. K. Phosphatidylinositol 3-kinase mutations identified in human cancer are oncogenic. *Proc. Natl. Acad. Sci. U.S.A.* **2005**, *102*, 802–807.

(32) Davies, S. P.; Reddy, H.; Caivano, M.; Cohen, P. Specificity and mechanism of action of some commonly used protein kinase inhibitors. *Biochem. J.* **2000**, *351*, 95–105.

(33) CYP450 inhibition was measured using a fluorescence based assay at BioFocus DPI.

(34) CYP450 induction was measured using fresh human hepatocytes in the Cloe Screen at Cyprotex.

(35) Measured using a whole cell patch clamp assay at BioFocus DPI.

(36) Workman, P.; Twentyman, P.; Balkwill, F. United Kingdom Coordinating Committee on Cancer Research Guidelines for the Welfare of Animals in Experimental Neoplasia. 2nd Ed. *Cancer* **1998**, *77*, 1–10.

(37) Eccles, S. A.; Court, W. J.; Box, G. A.; Dean, C. J.; Melton, R. G.; Springer, C. J. Regression of established breast carcinoma xenografts with antibody-directed enzyme prodrug therapy against c-erbB2 p185. *Cancer Res.* **1994**, *54*, 5171–5177.